CHAPTER 1

Introduction to FDTD

Computational electromagnetics (CEM) has evolved rapidly during the past decade to a point where now extremely accurate predictions can be given for a variety of electromagnetic problems, including the scattering cross-section of radar targets and the precise design of antennas and microwave devices. In general, commonly used CEM methods today can be classified into two categories. The first is based on differential equation (DE) methods, whereas the second is based on integral equation (IE) methods. Both IE and DE solution methods are based on the applications of Maxwell's equations and the appropriate boundary conditions associated with the problem to be solved. The IE methods in general provide approximations for IEs in terms of finite sums, whereas the DE methods provide approximations for DEs as finite differences.

In previous years, most numerical electromagnetic analysis has taken place in the frequency domain where time-harmonic behavior is assumed. Frequency domain was favored over time domain because a frequency-domain approach is more suitable for obtaining analytical solutions for canonical problems, which are used to verify the numerical results obtained as a first step before depending on a newly developed numerical method for generating data for real-world applications. Furthermore, the experimental hardware available for making measurements in past years was largely confined to the frequency-domain approach.

The recent development of faster and more powerful computational resources allowed for more advanced time-domain CEM models. More focus is directed toward DE time-domain approaches as they are easier to formulate and to adapt in computer simulation models without complex mathematics. They also provide more physical insight to the characteristics of the problems.

Therefore, an in-depth analysis and implementation of the commonly used time-domain DE approach, namely, the finite-difference time-domain (FDTD) method for CEM applications, is covered in this book, along with applications related to antenna designs, microwave filter designs, and radar cross-section analysis of three-dimensional targets.

The FDTD method has gained tremendous popularity in the past decade as a tool for solving Maxwell's equations. It is based on simple formulations that do not require complex asymptotic or Green's functions. Although it solves the problem in time, it can provide frequency-domain responses over a wide band using the Fourier transform. It can easily handle composite geometries consisting of different types of materials including dielectric,

magnetic, frequency-dependent, nonlinear, and anisotropic materials. The FDTD technique is easy to implement using parallel computation algorithms. These features of the FDTD method have made it the most attractive technique of CEM for many microwave devices and antenna applications.

FDTD has been used to solve numerous types of problems arising while studying many applications, including the following:

- scattering, radar cross-section
- microwave circuits, waveguides, fiber optics
- antennas (radiation, impedance)
- propagation
- medical applications
- shielding, coupling, electromagnetic compatibility (EMC), electromagnetic pulse (EMP) protection
- nonlinear and other special materials
- geological applications
- inverse scattering
- plasma

1.1 The finite-difference time-domain method basic equations

The starting point for the construction of an FDTD algorithm is Maxwell's time-domain equations. The differential time-domain Maxwell's equations needed to specify the field behavior over time are

$$\nabla \times \vec{H} = \frac{\partial \vec{D}}{\partial t} + \vec{J}, \tag{1.1a}$$

$$\nabla \times \vec{E} = -\frac{\partial \vec{B}}{\partial t} - \vec{M}, \tag{1.1b}$$

$$\nabla \cdot \vec{D} = \rho_e, \tag{1.1c}$$

$$\nabla \cdot \vec{B} = \rho_m, \tag{1.1d}$$

where $\vec{E}$ is the electric field strength vector in volts per meter, $\vec{D}$ is the electric displacement vector in coulombs per square meter, $\vec{H}$ is the magnetic field strength vector in amperes per meter, $\vec{B}$ is the magnetic flux density vector in webers per square meter, $\vec{J}$ is the electric current density vector in amperes per square meter, $\vec{M}$ is the magnetic current density vector in volts per square meter, ρ_e is the electric charge density in coulombs per cubic meter, and ρ_m is the magnetic charge density in webers per cubic meter.

Constitutive relations are necessary to supplement Maxwell's equations and characterize the material media. Constitutive relations for linear, isotropic, and nondispersive materials can be written as

$$\vec{D} = \varepsilon \vec{E}, \tag{1.2a}$$

$$\vec{B} = \mu \vec{H}, \tag{1.2b}$$

where ε is the permittivity, and μ is the permeability of the material. In free space

$$\varepsilon = \varepsilon_0 \approx 8.854 \times 10^{-12} \text{ farad/meter},$$

$$\mu = \mu_0 = 4\pi \times 10^{-7} \text{ henry/meter}.$$

We only need to consider curl equations (1.1a) and (1.1b) while deriving FDTD equations because the divergence equations can be satisfied by the developed FDTD updating equations [1]. The electric current density $\vec{J}$ is the sum of the conduction current density $\vec{J}_c = \sigma^e \vec{E}$ and the impressed current density $\vec{J}_i$ as $\vec{J} = \vec{J}_c + \vec{J}_i$. Similarly, for the magnetic current density, $\vec{M} = \vec{M}_c + \vec{M}_i$, where $\vec{M}_c = \sigma^m \vec{H}$. Here σ^e is the electric conductivity in siemens per meter, and σ^m is the magnetic conductivity in ohms per meter. Upon decomposing the current densities in (1.1) to conduction and impressed components and by using the constitutive relations (1.2) we can rewrite Maxwell's curl equations as

$$\nabla \times \vec{H} = \varepsilon \frac{\partial \vec{E}}{\partial t} + \sigma^e \vec{E} + \vec{J}_i, \tag{1.3a}$$

$$\nabla \times \vec{E} = -\mu \frac{\partial \vec{H}}{\partial t} - \sigma^m \vec{H} - \vec{M}_i. \tag{1.3b}$$

This formulation treats only the electromagnetic fields $\vec{E}$ and $\vec{H}$ and not the fluxes $\vec{D}$ and $\vec{B}$. All four constitutive parameters ε, μ, σ^e, and σ^m are present so that any linear isotropic material can be specified. Treatment of electric and magnetic sources is included through the impressed currents. Although only the curl equations are used and the divergence equations are not part of the FDTD formalism, the divergence equations can be used as a test on the predicted field response, so that after forming $\vec{D} = \varepsilon \vec{E}$ and $\vec{B} = \mu \vec{H}$ from the predicted $\vec{E}$ and $\vec{H}$ fields, the resulting $\vec{D}$ and $\vec{B}$ must satisfy the divergence equations.

Equation (1.3) is composed of two vector equations, and each vector equation can be decomposed into three scalar equations for three-dimensional space. Therefore, Maxwell's curl equations can be represented with the following six scalar equations in a Cartesian coordinate system (x, y, z):

$$\frac{\partial E_x}{\partial t} = \frac{1}{\varepsilon_x}\left(\frac{\partial H_z}{\partial y} - \frac{\partial H_y}{\partial z} - \sigma_x^e E_x - J_{ix}\right), \tag{1.4a}$$

$$\frac{\partial E_y}{\partial t} = \frac{1}{\varepsilon_y}\left(\frac{\partial H_x}{\partial z} - \frac{\partial H_z}{\partial x} - \sigma_y^e E_y - J_{iy}\right), \tag{1.4b}$$

$$\frac{\partial E_z}{\partial t} = \frac{1}{\varepsilon_z}\left(\frac{\partial H_y}{\partial x} - \frac{\partial H_x}{\partial y} - \sigma_z^e E_z - J_{iz}\right), \tag{1.4c}$$

$$\frac{\partial H_x}{\partial t} = \frac{1}{\mu_x}\left(\frac{\partial E_y}{\partial z} - \frac{\partial E_z}{\partial y} - \sigma_x^m H_x - M_{ix}\right), \tag{1.4d}$$

$$\frac{\partial H_y}{\partial t} = \frac{1}{\mu_y}\left(\frac{\partial E_z}{\partial x} - \frac{\partial E_x}{\partial z} - \sigma_y^m H_y - M_{iy}\right), \tag{1.4e}$$

$$\frac{\partial H_z}{\partial t} = \frac{1}{\mu_z}\left(\frac{\partial E_x}{\partial y} - \frac{\partial E_y}{\partial x} - \sigma_z^m H_z - M_{iz}\right). \tag{1.4f}$$

The material parameters ε_x, ε_y, and ε_z are associated with electric field components E_x, E_y, and E_z through constitutive relations $D_x = \varepsilon_x E_x$, $D_y = \varepsilon_y E_y$, and $D_z = \varepsilon_z E_z$, respectively. Similarly, the material parameters μ_x, μ_y, and μ_z are associated with magnetic field components H_x, H_y, and H_z through constitutive relations $B_x = \mu_x H_x$, $B_y = \mu_y H_y$, and $B_z = \mu_z H_z$, respectively. Similar decompositions for other orthogonal coordinate systems are possible, but they are less attractive from the applications point of view.

The FDTD algorithm divides the problem geometry into a spatial grid where electric and magnetic field components are placed at certain discrete positions in space, and it solves Maxwell's equations in time at discrete time instances. This can be implemented by first approximating the time and space derivatives appearing in Maxwell's equations by finite differences and next by constructing a set of equations that calculate the values of fields at a future time instant from the values of fields at a past time instant, therefore constructing a time marching algorithm that simulates the progression of the fields in time [2].

1.2 Approximation of derivatives by finite differences

An arbitrary continuous function can be sampled at discrete points, and the discrete function becomes a good approximation of the continuous function if the sampling rate is sufficient relative to the function's variation. Sampling rate determines the accuracy of operations performed on the discrete function that approximates the operations on the continuous functions as well. However, another factor that determines the accuracy of an operation on a discrete function is the choice of the discrete operator. Most of the time it is possible to use more than one way of performing an operation on a discrete function. Here we will consider the derivative operation.

Consider the continuous function given in Figure 1.1(a–c), sampled at discrete points. The expression for the derivative of $f(x)$ at point x can be written as

$$f'(x) = \lim_{\Delta x \to 0} \frac{f(x + \Delta x) - f(x)}{\Delta x}. \tag{1.5}$$

However, since Δx is a nonzero fixed number, the derivative of $f(x)$ can be approximately taken as

$$f'(x) \approx \frac{f(x + \Delta x) - f(x)}{\Delta x}. \tag{1.6}$$

The derivative of $f(x)$ is the slope of the dashed line as illustrated in Figure 1.1(a). Equation (1.6) is called the *forward difference* formula since one forward point $f(x + \Delta x)$ is used to evaluate $f'(x)$ together with $f(x)$.

It is evident that another formula for an approximate $f'(x)$ can be obtained by using a backward point $f(x - \Delta x)$ rather than the forward point $f(x + \Delta x)$ as illustrated in Figure 1.1(b), which can be written as

$$f'(x) \approx \frac{f(x) - f(x - \Delta x)}{\Delta x}. \tag{1.7}$$

This equation is called the *backward difference* formula due to the use of the backward point $f(x - \Delta x)$.

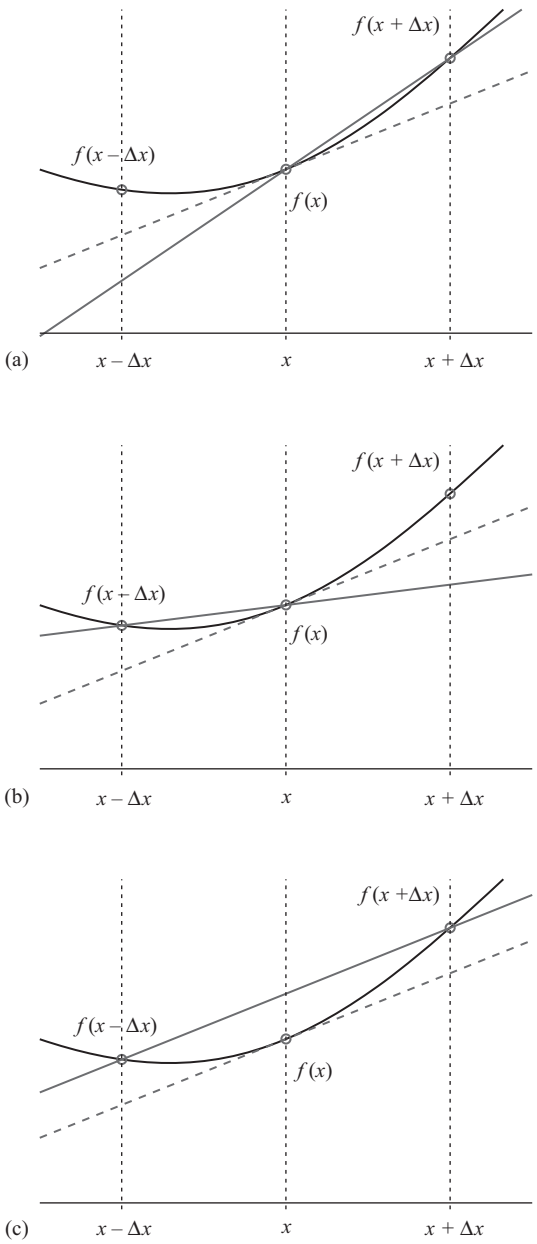

Figure 1.1 (a) Approximation of the derivative of $f(x)$ at x by finite differences: forward difference; (b) approximation of the derivative of $f(x)$ at x by finite differences: backward difference; (c) approximation of the derivative of $f(x)$ at x by finite differences: central difference.

The third way of obtaining a formula for an approximate $f'(x)$ is by averaging the forward difference and backward difference formulas, such that

$$f'(x) \approx \frac{f(x+\Delta x) - f(x-\Delta x)}{\Delta x}. \tag{1.8}$$

Equation (1.8) is called the *central difference* formula since both the forward and backward points around the center are used. The line representing the derivative of $f(x)$ calculated using the central difference formula is illustrated in Figure 1.1(c). It should be noted that the value of the function $f(x)$ at x is not used in central difference formula.

Examination of Figure 1.1 immediately reveals that the three different schemes yield different values for $f'(x)$, with an associated amount of error. The amount of error introduced by these difference formulas can be evaluated analytically by using the Taylor series approach. For instance, the Taylor series expansion of $f(x+\Delta x)$ can be written as

$$f(x+\Delta x) = f(x) + \Delta x f'(x) + \frac{(\Delta x)^2}{2} f''(x) + \frac{(\Delta x)^3}{6} f'''(x) + \frac{(\Delta x)^4}{24} f''''(x) + \cdots. \tag{1.9}$$

This equation gives an exact expression for $f(x+\Delta x)$ as a series in terms of Δx and derivatives of $f(x)$, if $f(x)$ satisfies certain conditions and infinite number of terms, theoretically, are being used. Equation (1.9) can be rearranged to express $f'(x)$ as

$$f'(x) = \frac{f(x+\Delta x) - f(x)}{\Delta x} - \frac{\Delta x}{2} f''(x) - \frac{(\Delta x)^2}{6} f'''(x) - \frac{(\Delta x)^3}{24} f''''(x) - \cdots. \tag{1.10}$$

Here it can be seen that the first term on the right-hand side of (1.10) is the same as the forward difference formula given by (1.6). The sum of the rest of the terms is the difference between the approximate derivative given by the forward difference formula and the exact derivative $f'(x)$, and hence is the amount of error introduced by the forward difference formula. Equation (1.10) can be rewritten as

$$f'(x) = \frac{f(x+\Delta x) - f(x)}{\Delta x} + O(\Delta x), \tag{1.11}$$

where $O(\Delta x)$ represents the error term. The most significant term in $O(\Delta x)$ is $\Delta x/2$, and the order of Δx in this most significant term is one. Therefore, the forward difference formula is *first-order accurate*. The interpretation of first-order accuracy is that the most significant term in the error introduced by a first-order accurate formula is proportional to the sampling period. For instance, if the sampling period is decreased by half, the error reduces by half.

A similar analysis can be performed for evaluation of the error of the backward formula starting with the Taylor series expansion of $f(x-\Delta x)$.

$$f(x-\Delta x) = f(x) - \Delta x f'(x) + \frac{(\Delta x)^2}{2} f''(x) - \frac{(\Delta x)^3}{6} f'''(x) + \frac{(\Delta x)^4}{24} f''''(x) + \cdots. \tag{1.12}$$

This equation can be rearranged to express $f'(x)$ as

$$f'(x) = \frac{f(x) - f(x - \Delta x)}{\Delta x} + \frac{\Delta x}{2} f''(x) - \frac{(\Delta x)^2}{6} f'''(x) + \frac{(\Delta x)^3}{24} f''''(x) - \cdots. \tag{1.13}$$

The first term on the right-hand side of (1.13) is the same as the backward difference formula and the sum of the rest of the terms represents the error introduced by the backward difference formula to the exact derivative of $f(x)$, such that

$$f'(x) = \frac{f(x) - f(x - \Delta x)}{\Delta x} + O(\Delta x). \tag{1.14}$$

The order of Δx in the most significant term of $O(\Delta x)$ is one; hence the backward difference formula is *first-order accurate*.

The difference between the Taylor series expansions of $f(x + \Delta x)$ and $f(x - \Delta x)$ can be expressed using (1.9) and (1.12) as

$$f(x + \Delta x) - f(x - \Delta x) = 2\Delta x f'(x) + \frac{2(\Delta x)^3}{6} f'''(x) + \cdots. \tag{1.15}$$

This equation can be rearranged to express $f'(x)$ as

$$f'(x) = \frac{f(x + \Delta x) - f(x - \Delta x)}{2\Delta x} - \frac{(\Delta x)^2}{6} f'''(x) + \cdots = \frac{f(x + \Delta x) - f(x - \Delta x)}{2\Delta x} + O\Big((\Delta x)^2\Big), \tag{1.16}$$

where the first term on right-hand side is the same as the central difference formula given in (1.8) and the order of Δx in the most significant term of the error $O((\Delta x)^2)$ is two; hence the central difference formula is *second-order accurate*. The interpretation of second-order accuracy is that the most significant term in the error introduced by a second-order accurate formula is proportional to the square of sampling period. For instance, if the sampling period is decreased by half, the error is reduced by a factor of four. Hence, a second-order accurate formula such as the central difference formula is more accurate than a first-order accurate formula.

For an example, consider a function $f(x) = \sin(x)e^{-0.3x}$ as displayed in Figure 1.2(a). The exact first-order derivative of this function is

$$f'(x) = \cos(x)e^{-0.3x} - 0.3\sin(x)e^{-0.3x}.$$

This function $f(x)$ is sampled with a sampling period $\Delta x = \pi/5$, and approximate derivatives are calculated for $f(x)$ using the forward difference, backward difference, and central difference formulas. The derivative of the function $f'(x)$ and its finite difference approximations are plotted in Figure 1.2(b). The errors introduced by the difference formulas, which are the differences between $f'(x)$ and its finite difference approximations, are plotted in Figure 1.2(c) for the sampling interval $\Delta x = \pi/5$. It is evident that the error introduced by the central difference formula is smaller than the errors introduced by the forward difference

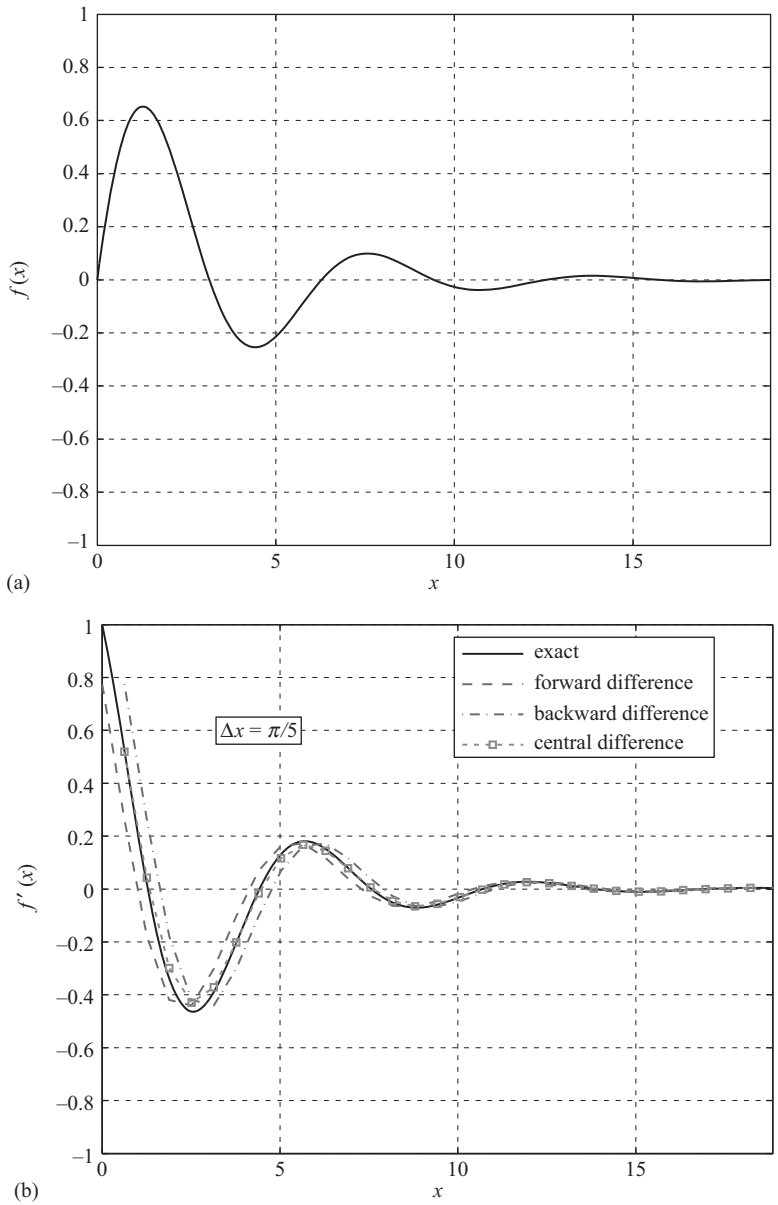

Figure 1.2 (a) $f(x), f'(x)$, and differences between $f'(x)$ and finite difference approximations of $f'(x)$ for $\Delta x = \pi/5$ and $\Delta x = \pi/10$: $f(x) = \sin(x)e^{-0.3x}$; (b) $f(x), f'(x)$, and differences between $f'(x)$ and finite difference approximations of $f'(x)$ for $\Delta x = \pi/5$ and $\Delta x = \pi/10$: $f'(x) = \cos(x)e^{-0.3x} - 0.3\sin(x)e^{-0.3x}$ and finite difference approximations of $f'(x)$ for $\Delta x = \pi/5$; (c) $f(x), f'(x)$, and differences between $f'(x)$ and finite difference approximations of $f'(x)$ for $\Delta x = \pi/5$ and $\Delta x = \pi/10$: error($f'(x)$) for $\Delta x = \pi/5$; (d) $f(x), f'(x)$, and differences between $f'(x)$ and finite difference approximations of $f'(x)$ for $\Delta x = \pi/5$ and $\Delta x = \pi/10$: error($f'(x)$) for $\Delta x = \pi/10$.

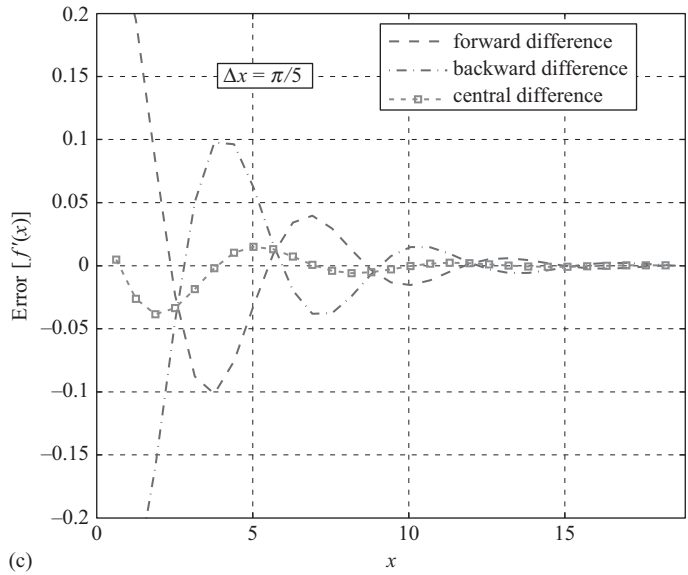

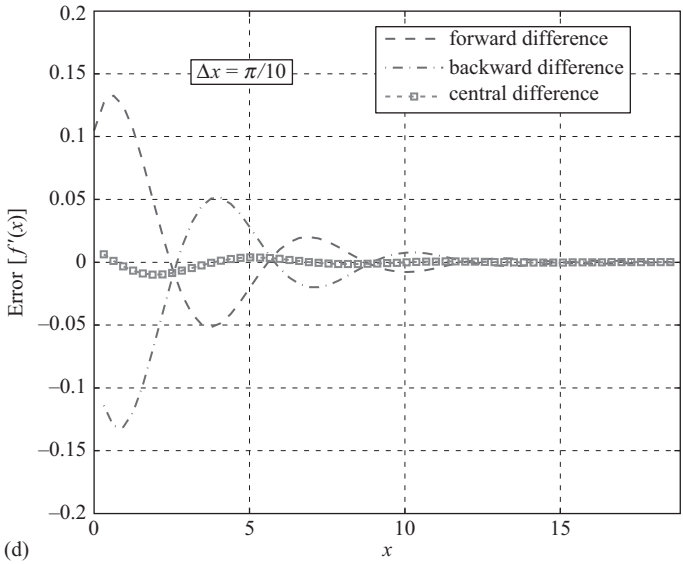

Figure 1.2 (*Continued*)

and backward difference formulas. Furthermore, the errors introduced by the difference formulas for the sampling period $\Delta x = \pi/10$ are plotted in Figure 1.2(d). It can be realized that as the sampling period is halved, the errors of the forward difference and backward difference formulas are halved as well, and the error of the central difference formula is reduced by a factor of four.

The MATLAB® code calculating $f(x)$ and its finite difference derivatives, and generating the plots in Figure 1.2 is shown in Listing 1.1.

Listing 1.1 MATLAB code generating Figure 1.2(a–d)

```
% create exact function and its derivative
N_exact = 301; % number of sample points for exact function
x_exact = linspace(0,6*pi,N_exact);
f_exact = sin(x_exact).*exp(-0.3*x_exact);
f_derivative_exact = cos(x_exact).*exp(-0.3*x_exact) ...
                     -0.3*sin(x_exact).*exp(-0.3*x_exact);

% plot exact function
figure(1);
plot(x_exact,f_exact,'k-','linewidth',1.5);
set (gca,'FontSize',12,'fontweight','demi');
axis([0 6*pi -1 1]); grid on;
xlabel('$x$','Interpreter','latex','FontSize',16);
ylabel('$f(x)$','Interpreter','latex','FontSize',16);

% create exact function for pi/5 sampling period
% and its finite difference derivatives
N_a = 31; % number of points for pi/5 sampling period
x_a = linspace(0,6*pi,N_a);
f_a = sin(x_a).*exp(-0.3*x_a);
f_derivative_a = cos(x_a).*exp(-0.3*x_a) ...
                 -0.3*sin(x_a).*exp(-0.3*x_a);

dx_a = pi/5;
f_derivative_forward_a  = zeros(1,N_a);
f_derivative_backward_a = zeros(1,N_a);
f_derivative_central_a  = zeros(1,N_a);
f_derivative_forward_a(1:N_a-1) = ...
        (f_a(2:N_a)-f_a(1:N_a-1))/dx_a;
f_derivative_backward_a(2:N_a) = ...
        (f_a(2:N_a)-f_a(1:N_a-1))/dx_a;
f_derivative_central_a(2:N_a-1) = ...
        (f_a(3:N_a)-f_a(1:N_a-2))/(2*dx_a);


% create exact function for pi/10 sampling period
% and its finite difference derivatives
N_b = 61; % number of points for pi/10 sampling period
x_b = linspace(0,6*pi,N_b);
f_b = sin(x_b).*exp(-0.3*x_b);
f_derivative_b = cos(x_b).*exp(-0.3*x_b) ...
                 -0.3*sin(x_b).*exp(-0.3*x_b);
dx_b = pi/10;
f_derivative_forward_b  = zeros(1,N_b);
f_derivative_backward_b = zeros(1,N_b);
f_derivative_central_b  = zeros(1,N_b);
f_derivative_forward_b(1:N_b-1) = ...
        (f_b(2:N_b)-f_b(1:N_b-1))/dx_b;
f_derivative_backward_b(2:N_b) = ...
        (f_b(2:N_b)-f_b(1:N_b-1))/dx_b;
f_derivative_central_b(2:N_b-1) = ...
        (f_b(3:N_b)-f_b(1:N_b-2))/(2*dx_b);

```

```
% plot exact derivative of the function and its finite difference
% derivatives using pi/5 sampling period
figure(2);
plot(x_exact,f_derivative_exact,'k', ...
    x_a(1:N_a-1),f_derivative_forward_a(1:N_a-1),'b--', ...
    x_a(2:N_a),f_derivative_backward_a(2:N_a),'r-.', ...
    x_a(2:N_a-1),f_derivative_central_a(2:N_a-1),':ms', ...
    'MarkerSize',4, 'linewidth',1.5);
set (gca,'FontSize',12,'fontweight','demi');
axis([0 6*pi -1 1]);
grid on;
legend('exact', 'forward difference',...
    'backward difference','central difference');
xlabel('$x$','Interpreter','latex','FontSize',16);
ylabel('$f''(x)$','Interpreter','latex','FontSize',16);
text(pi,0.6,'$\Delta x = \pi/5$','Interpreter', ...
    'latex','fontsize',16, 'BackgroundColor','w','EdgeColor','k');

% plot error for finite difference derivatives
% using pi/5 sampling period
error_forward_a  = f_derivative_a - f_derivative_forward_a;
error_backward_a = f_derivative_a - f_derivative_backward_a;
error_central_a  = f_derivative_a - f_derivative_central_a;

figure(3);
plot(x_a(1:N_a-1),error_forward_a(1:N_a-1),'b--', ...
    x_a(2:N_a),error_backward_a(2:N_a),'r-.', ...
    x_a(2:N_a-1),error_central_a(2:N_a-1),':ms', ...
    'MarkerSize',4, 'linewidth',1.5);

set (gca,'FontSize',12,'fontweight','demi');
axis([0 6*pi -0.2 0.2]);
grid on;
legend('forward difference', 'backward difference', ...
    'central difference');
xlabel('$x$','Interpreter','latex','FontSize',16);
ylabel('error $[f''(x)]$','Interpreter','latex','FontSize',16);
text(pi,0.15,'$\Delta x = \pi/5$','Interpreter', ...
    'latex','fontsize',16, 'BackgroundColor','w','EdgeColor','k');

% plot error for finite difference derivatives
% using pi/10 sampling period
error_forward_b  = f_derivative_b - f_derivative_forward_b;
error_backward_b = f_derivative_b - f_derivative_backward_b;
error_central_b  = f_derivative_b - f_derivative_central_b;

figure(4);
plot(x_b(1:N_b-1),error_forward_b(1:N_b-1),'b-- , ...
    x_b(2:N_b),error_backward_b(2:N_b),'r-.', ...
    x_b(2:N_b-1),error_central_b(2:N_b-1),':ms', ...
    'MarkerSize',4, 'linewidth',1.5);

set (gca,'FontSize',12,'fontweight','demi');
```

```
axis([0 6*pi -0.2 0.2]);
grid on;
legend('forward difference','backward difference', ...
    'central difference');
xlabel('$x$','Interpreter','latex','FontSize',16);
ylabel('error $[f''(x)]$','Interpreter','latex','FontSize',16);
text(pi,0.15,'$\Delta x = \pi/10$','Interpreter', ...
    'latex','fontsize',16,'BackgroundColor','w','EdgeColor','k');
```

Values of the function $f(x)$ at two neighboring points around x have been used to obtain a second-order accurate central difference formula to approximate $f'(x)$. It is possible to obtain formulas with higher orders of accuracy by including a larger number of neighboring points in the derivation of a formula for $f'(x)$. However, although there are FDTD formulations developed based on higher-order accurate formulas, the conventional FDTD is based on the second-order accurate central difference formula, which is found to be sufficiently accurate for most electromagnetics applications and simple in implementation and understanding.

It is possible to obtain finite-difference formulas for approximating higher-order derivatives as well. For instance, if we take the sum of the Taylor series expansions of $f(x + \Delta x)$ and $f(x - \Delta x)$ using (1.9) and (1.12), we obtain

$$f(x+\Delta x)+f(x-\Delta x)=2f(x)+(\Delta x)^2 f''(x)+\frac{(\Delta x)^4}{12}f''''(x)+\cdots. \tag{1.17}$$

After rearranging the equation to have $f''(x)$ on the left-hand side, we get

$$\begin{aligned} f''(x) &= \frac{f(x+\Delta x)-2f(x)+f(x-\Delta x)}{(\Delta x)^2}-\frac{(\Delta x)^2}{12}f''''(x)+\cdots \\ &= \frac{f(x+\Delta x)-2f(x)+f(x-\Delta x)}{(\Delta x)^2}+O\big((\Delta x)^2\big). \end{aligned} \tag{1.18}$$

Using (1.18) we can obtain a central difference formula for the second-order derivative $f''(x)$ as

$$f''(x)\approx\frac{f(x+\Delta x)-2f(x)+f(x-\Delta x)}{(\Delta x)^2}, \tag{1.19}$$

which is second-order accurate due to $O(\Delta x)^2$.

Similarly, some other finite difference formulas can be obtained for the first- and second-order derivatives with different orders of accuracy based on different sampling points. A list of finite difference formulas is given for the first- and second-order derivatives in Table 1.1 as a reference (Figure 1.3).

Table 1.1 Finite difference formulas for the first- and second-order derivatives where the function f with the subscript i is an abbreviation of $f(x)$. Similar notation can be implemented for $f(x + \Delta x)$, $f(x + 2\Delta x)$, etc., as shown in Figure 1.3. FD, forward difference; BD, backward difference; CD, central difference.

Derivative $\partial f/\partial x$		Derivative $\partial^2 f/\partial x^2$	
Difference scheme	**Type error**	**Difference scheme**	**Type error**
$\dfrac{f_{i+1} - f_i}{\Delta x}$	FD $O(\Delta x)$	$\dfrac{f_{i+2} - 2f_{i+1} + f_i}{(\Delta x)^2}$	FD $O(\Delta x)$
$\dfrac{f_i - f_{i-1}}{\Delta x}$	BD $O(\Delta x)$	$\dfrac{f_{i+2} - 2f_{i-1} + f_{i-2}}{(\Delta x)^2}$	BD $O(\Delta x)$
$\dfrac{f_{i+1} - f_{i-1}}{2\Delta x}$	CD $O((\Delta x)^2)$	$\dfrac{f_{i+1} - 2f_i + f_{i-1}}{(\Delta x)^2}$	CD $O((\Delta x)^2)$
$\dfrac{-f_{i+2} + 4f_{i+1} - 3f_i}{2\Delta x}$	FD $O((\Delta x)^2)$	$\dfrac{-f_{i+2} + 16f_{i+1} - 30f_i + 16f_{i-1} - f_{i-2}}{12(\Delta x)^2}$	CD $O((\Delta x)^4)$
$\dfrac{3f_{i+1} - 4f_{i-1} + f_{i-2}}{2\Delta x}$	BD $O((\Delta x)^2)$		
$\dfrac{-f_{i+2} + 8f_{i+1} - 8f_{i-1} + f_{i-2}}{12\Delta x}$	CD $O((\Delta x)^4)$		

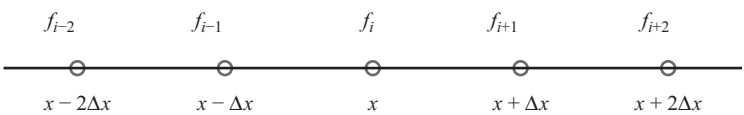

Figure 1.3 Sample points of $f(x)$.

1.3 FDTD updating equations for three-dimensional problems

In 1966, Yee originated a set of finite-difference equations for the time-dependent Maxwell's curl equations system [2]. These equations can be represented in discrete form, both in space and time, employing the second-order accurate central difference formula. As mentioned before, the electric and magnetic field components are sampled at discrete positions both in time and space. The FDTD technique divides the three-dimensional problem geometry into cells to form a grid. Figure 1.4 illustrates an FDTD grid composed of $(N_x \times N_y \times N_z)$ cells. A unit cell of this grid is called a Yee cell. Using rectangular Yee cells, a stepped or "staircase" approximation of the surface and internal geometry of the structure of interest is made with a space resolution set by the size of the unit cell.

The discrete spatial positions of the field components have a specific arrangement in the Yee cell, as demonstrated in Figure 1.5. The electric field vector components are placed at

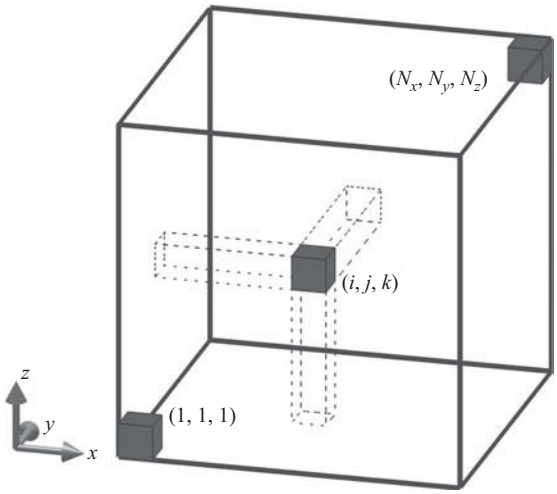

Figure 1.4 A three-dimensional FDTD computational space composed of $(N_x \times N_y \times N_z)$ Yee cells.

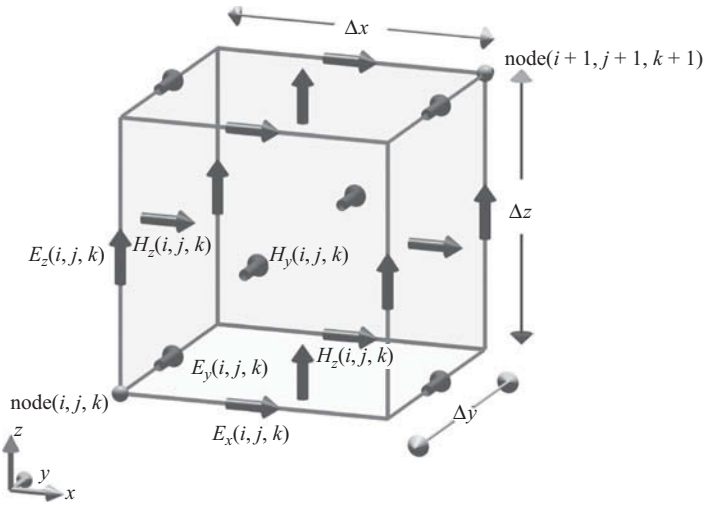

Figure 1.5 Arrangement of field components on a Yee cell indexed as (i, j, k).

the centers of the edges of the Yee cells and oriented parallel to the respective edges, and the magnetic field vector components are placed at the centers of the faces of the Yee cells and are oriented normal to the respective faces. This provides a simple picture of three-dimensional space being filled by an interlinked array of Faraday's law and Ampere's law contours. It can be easily noticed in Figure 1.5 that each magnetic field vector is surrounded

by four electric field vectors that are curling around the magnetic field vector, thus simulating Faraday's law. Similarly, if the neighboring cells are also added to the picture, it would be apparent that each electric field vector is surrounded by four magnetic field vectors that are curling around the electric field vector, thus simulating Ampere's law.

Figure 1.5 shows the indices of the field components, which are indexed as (i, j, k), associated with a cell indexed as (i, j, k). For a computational domain composed of uniform Yee cells having dimension Δx in the x direction, Δy in the y direction, and Δz in the z direction, the actual positions of the field components with respect to an origin coinciding with the position of the node (1, 1, 1) can easily be calculated as

$$\begin{aligned}
E_x(i,j,k) &\Rightarrow ((i-0.5)\Delta x,\ (j-1)\Delta y,\ (k-1)\Delta z),\\
E_y(i,j,k) &\Rightarrow ((i-1)\Delta x,\ (j-0.5)\Delta y,\ (k-1)\Delta z),\\
E_z(i,j,k) &\Rightarrow ((i-1)\Delta x,\ (j-1)\Delta y,\ (k-0.5)\Delta z),\\
H_x(i,j,k) &\Rightarrow ((i-1)\Delta x,\ (j-0.5)\Delta y,\ (k-0.5)\Delta z),\\
H_y(i,j,k) &\Rightarrow ((i-0.5)\Delta x,\ (j-1)\Delta y,\ (k-0.5)\Delta z),\\
H_z(i,j,k) &\Rightarrow ((i-0.5)\Delta x,\ (j-0.5)\Delta y,\ (k-1)\Delta z).
\end{aligned}$$

The FDTD algorithm samples and calculates the fields at discrete time instants; however, the electric and magnetic field components are not sampled at the same time instants. For a time-sampling period Δt, the electric field components are sampled at time instants $0,\ \Delta t,\ 2\Delta t,\ \ldots,\ n\Delta t,\ \ldots$; however, the magnetic field components are sampled at time instants $\frac{1}{2}\Delta t, (1+\frac{1}{2})\Delta t, \ldots, (n+\frac{1}{2})\Delta t, \ldots$. Therefore, the electric field components are calculated at integer time steps, and magnetic field components are calculated at half-integer time steps, and they are offset from each other by $\Delta t/2$. The field components need to be referred not only by their spatial indices which indicate their positions in space, but also by their temporal indices, which indicate their time instants. Therefore, a superscript notation is adopted to indicate the time instant. For instance, the z component of an electric field vector positioned at $((i-1)\Delta x, (j-1)\Delta y, (k-0.5)\Delta z)$ and sampled at time instant $n\Delta t$ is referred to as $E_z^n(i,j,k)$. Similarly, the y component of a magnetic field vector positioned at $((i-0.5)\Delta x, (j-1)\Delta y, (k-0.5)\Delta z)$ and sampled at time instant $(n+\frac{1}{2})\Delta t$ is referred to as $H_y^{n+1/2}(i,j,k)$.

The material parameters (permittivity, permeability, electric, and magnetic conductivities) are distributed over the FDTD grid and are associated with field components; therefore, they are indexed the same as their respective field components. For instance, Figure 1.6 illustrates the indices for the permittivity and permeability parameters. The electric conductivity is distributed and indexed the same as the permittivity, and the magnetic conductivity is distributed and indexed the same as the permeability.

Having adopted an indexing scheme for the discrete samples of field components in both time and space, Maxwell's curl equations (1.4) that are given in scalar form can be expressed in terms of finite differences. For instance, consider again (1.4a):

$$\frac{\partial E_x}{\partial t} = \frac{1}{\varepsilon_x}\left(\frac{\partial H_z}{\partial y} - \frac{\partial H_y}{\partial z} - \sigma_x^e E_x - J_{ix}\right).$$

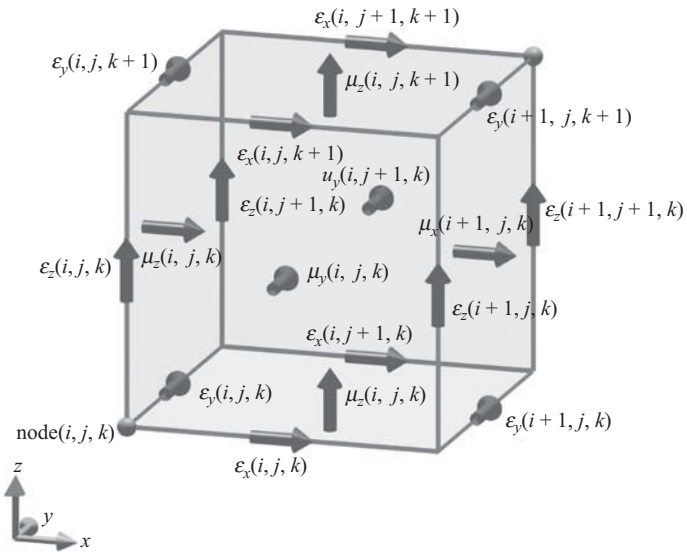

Figure 1.6 Material parameters indexed on a Yee cell.

The derivatives in this equation can be approximated by using the central difference formula with the position of $E_x(i,\ j,\ k)$ being the center point for the central difference formula in space and time instant $(n+\frac{1}{2})\Delta t$ as being the center point in time. Considering the field component positions given in Figure 1.7, we can write

$$\frac{E_x^{n+1}(i,j,k)-E_x^{n}(i,j,k)}{\Delta t}=\frac{1}{\varepsilon_x(i,j,k)}\frac{H_z^{n+\frac{1}{2}}(i,j,k)-H_z^{n+\frac{1}{2}}(i,j-1,k)}{\Delta y}$$
$$-\frac{1}{\varepsilon_x(i,j,k)}\frac{H_y^{n+\frac{1}{2}}(i,j,k)-H_y^{n+\frac{1}{2}}(i,j,k-1)}{\Delta z}$$
$$-\frac{\sigma_x^{e}(i,j,k)}{\varepsilon_x(i,j,k)}E_x^{n+\frac{1}{2}}(i,j,k)-\frac{1}{\varepsilon_x(i,j,k)}J_{ix}^{n+\frac{1}{2}}(i,j,k). \qquad (1.20)$$

It has already been mentioned that the electric field components are defined at integer time steps; however, the right-hand side of (1.20) includes an electric field term at time instant $(n+\frac{1}{2})\Delta t$, that is, $E_x^{n+1/2}(i,j,k)$. This term can be written as the average of the terms at time instants $(n+1)\Delta t$ and $n\Delta t$, such that

$$E_x^{n+\frac{1}{2}}(i,j,k)=\frac{E_x^{n+1}(i,j,k)+E_x^{n}(i,j,k)}{2}. \qquad (1.21)$$

Using (1.21) in (1.20) and arranging the terms such that the future term $E_x^{n+1}(i,j,k)$ is kept on the left side of the equation and the rest of the terms are moved to the right-hand side of the equation, we can write

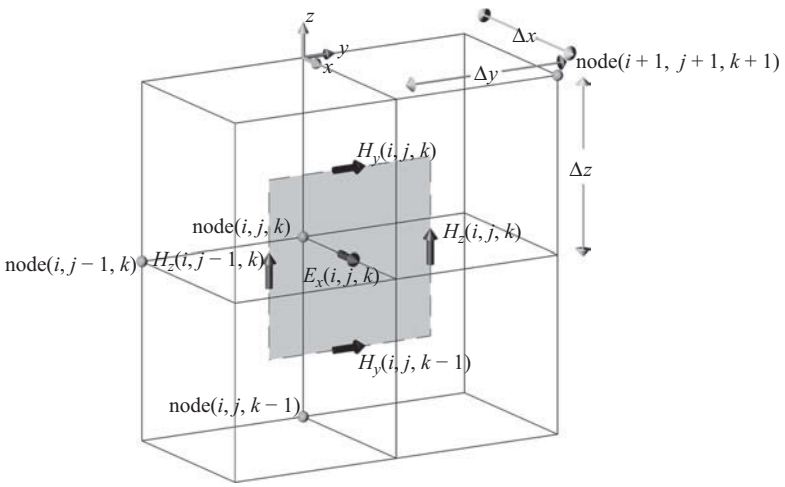

Figure 1.7 Field components around $E_x(i, j, k)$.

$$\frac{2\varepsilon_x(i,j,k)+\Delta t\sigma_x^e(i,j,k)}{2\varepsilon_x(i,j,k)}E_x^{n+1}(i,j,k)=\frac{2\varepsilon_x(i,j,k)-\Delta t\sigma_x^e(i,j,k)}{2\varepsilon_x(i,j,k)}E_x^{n}(i,j,k)$$
$$+\frac{\Delta t}{\varepsilon_x(i,j,k)\Delta y}\left(H_z^{n+\frac{1}{2}}(i,j,k)-H_z^{n+\frac{1}{2}}(i,j-1,k)\right)$$
$$-\frac{\Delta t}{\varepsilon_x(i,j,k)\Delta z}\left(H_y^{n+\frac{1}{2}}(i,j,k)-H_y^{n+\frac{1}{2}}(i,j,k-1)\right)$$
$$-\frac{\Delta t}{\varepsilon_x(i,j,k)}J_{ix}^{n+\frac{1}{2}}(i,j,k) \tag{1.22}$$

After some manipulations, we get

$$E_x^{n+1}(i,j,k)=\frac{2\varepsilon_x(i,j,k)-\Delta t\sigma_x^e(i,j,k)}{2\varepsilon_x(i,j,k)+\Delta t\sigma_x^e(i,j,k)}E_x^{n}(i,j,k)$$
$$+\frac{2\Delta t}{\left(2\varepsilon_x(i,j,k)+\Delta t\sigma_x^e(i,j,k)\right)\Delta y}\left(H_z^{n+\frac{1}{2}}(i,j,k)-H_z^{n+\frac{1}{2}}(i,j-1,k)\right)$$
$$-\frac{2\Delta t}{\left(2\varepsilon_x(i,j,k)+\Delta t\sigma_x^e(i,j,k)\right)\Delta z}\left(H_y^{n+\frac{1}{2}}(i,j,k)-H_y^{n+\frac{1}{2}}(i,j,k-1)\right)$$
$$-\frac{2\Delta t}{2\varepsilon_x(i,j,k)+\Delta t\sigma_x^e(i,j,k)}J_{ix}^{n+\frac{1}{2}}(i,j,k). \tag{1.23}$$

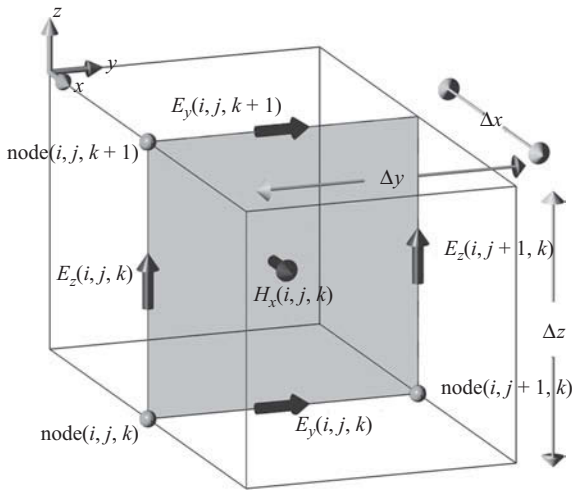

Figure 1.8 Field components around $H_x(i, j, k)$.

The form of (1.23) demonstrates how the future value of an electric field component can be calculated by using the past values of the electric field component, the magnetic field components, and the source components. This form of an equation is called an FDTD *updating equation*. Updating equations can easily be obtained for calculating $E_y^{n+1}(i,j,k)$ starting from (1.4b) and $E_z^{n+1}(i,j,k)$ starting from (1.4c) following the same methodology that has been used to obtain (1.23).

Similarly, updating equations can be obtained for magnetic field components following the same methodology. However, while applying the central difference formula to the time derivative of the magnetic field components, the central point in time shall be taken as $n\Delta t$. For instance, (1.4c), which is

$$\frac{\partial H_x}{\partial t} = \frac{1}{\mu_x}\left(\frac{\partial E_y}{\partial z} - \frac{\partial E_z}{\partial y} - \sigma_x^m H_x - M_{ix}\right),$$

can be approximated using finite differences based on the field positions (as shown in Figure 1.8) as

$$\begin{aligned}\frac{H_x^{n+\frac{1}{2}}(i,j,k) - H_x^{n-\frac{1}{2}}(i,j,k)}{\Delta t} &= \frac{1}{\mu_x(i,j,k)}\frac{E_y^n(i,j,k+1) - E_y^n(i,j,k)}{\Delta z} \\ &\quad - \frac{1}{\mu_x(i,j,k)}\frac{E_z^n(i,j+1,k) - E_z^n(i,j,k)}{\Delta y} \\ &\quad - \frac{\sigma_x^m(i,j,k)}{\mu_x(i,j,k)}H_x^n(i,j,k) - \frac{1}{\mu_x(i,j,k)}M_{ix}^n(i,j,k). \qquad (1.24)\end{aligned}$$

After some manipulations, the future term $H_x^{n+\frac{1}{2}}(i,j,k)$ in (1.24) can be moved to the left-hand side and the other terms can be moved to the right-hand side such that

$$\begin{aligned} H_x^{n+\frac{1}{2}}(i,j,k) = {} & \frac{2\mu_x(i,j,k) - \Delta t\sigma_x^m(i,j,k)}{2\mu_x(i,j,k) + \Delta t\sigma_x^m(i,j,k)} H_x^{n-\frac{1}{2}}(i,j,k) \\ & + \frac{2\Delta t}{\big(2\mu_x(i,j,k) + \Delta t\sigma_x^m(i,j,k)\big)\Delta z}\Big(E_y^n(i,j,k+1) - E_y^n(i,j,k)\Big) \\ & - \frac{2\Delta t}{\big(2\mu_x(i,j,k) + \Delta t\sigma_x^m(i,j,k)\big)\Delta y}\big(E_z^n(i,j+1,k) - E_z^n(i,j,k)\big) \\ & - \frac{2\Delta t}{2\mu_x(i,j,k) + \Delta t\sigma_x^m(i,j,k)} M_{ix}^n(i,j,k). \end{aligned} \tag{1.25}$$

This equation is the updating equation for $H_x^{n+\frac{1}{2}}(i,j,k)$. Similarly, updating equations can easily be obtained for $H_y^{n+\frac{1}{2}}(i,j,k)$ starting from (1.4e) and $H_z^{n+\frac{1}{2}}(i,j,k)$ starting from (1.4f) following the same methodology used to obtain (1.25).

Finally, (1.4a)–(1.4f) can be expressed using finite differences and can be arranged to construct the following six FDTD updating equations for the six components of electromagnetic fields by introduction of respective coefficient terms:

$$\begin{aligned} E_x^{n+1}(i,j,k) = {} & C_{exe}(i,j,k) \times E_x^n(i,j,k) \\ & + C_{exhz}(i,j,k) \times \Big(H_z^{n+\frac{1}{2}}(i,j,k) - H_z^{n+\frac{1}{2}}(i,j-1,k)\Big) \\ & + C_{exhy}(i,j,k) \times \Big(H_y^{n+\frac{1}{2}}(i,j,k) - H_y^{n+\frac{1}{2}}(i,j,k-1)\Big) \\ & + C_{exj}(i,j,k) \times J_{ix}^{n+\frac{1}{2}}(i,j,k), \end{aligned} \tag{1.26}$$

where

$$\begin{aligned} C_{exe}(i,j,k) &= \frac{2\varepsilon_x(i,j,k) - \Delta t\sigma_x^e(i,j,k)}{2\varepsilon_x(i,j,k) + \Delta t\sigma_x^e(i,j,k)}, \\ C_{exhz}(i,j,k) &= \frac{2\Delta t}{\big(2\varepsilon_x(i,j,k) + \Delta t\sigma_x^e(i,j,k)\big)\Delta y}, \\ C_{exhy}(i,j,k) &= -\frac{2\Delta t}{\big(2\varepsilon_x(i,j,k) + \Delta t\sigma_x^e(i,j,k)\big)\Delta z}, \\ C_{exj}(i,j,k) &= -\frac{2\Delta t}{2\varepsilon_x(i,j,k) + \Delta t\sigma_x^e(i,j,k)}. \end{aligned} \tag{1.27}$$

$$\begin{aligned} E_y^{n+1}(i,j,k) = {} & C_{eye}(i,j,k) \times E_y^n(i,j,k) \\ & + C_{eyhx}(i,j,k) \times \Big(H_x^{n+\frac{1}{2}}(i,j,k) - H_x^{n+\frac{1}{2}}(i,j,k-1)\Big) \\ & + C_{eyhz}(i,j,k) \times \Big(H_z^{n+\frac{1}{2}}(i,j,k) - H_z^{n+\frac{1}{2}}(i-1,j,k)\Big) \\ & + C_{eyj}(i,j,k) \times J_{iy}^{n+\frac{1}{2}}(i,j,k), \end{aligned}$$

where

$$
\begin{aligned}
C_{eye}(i,j,k) &= \frac{2\varepsilon_y(i,j,k) - \Delta t\sigma_y^e(i,j,k)}{2\varepsilon_y(i,j,k) + \Delta t\sigma_y^e(i,j,k)},\\
C_{eyhx}(i,j,k) &= \frac{2\Delta t}{\Big(2\varepsilon_y(i,j,k) + \Delta t\sigma_y^e(i,j,k)\Big)\Delta z},\\
C_{eyhz}(i,j,k) &= -\frac{2\Delta t}{\Big(2\varepsilon_y(i,j,k) + \Delta t\sigma_y^e(i,j,k)\Big)\Delta x},\\
C_{eyj}(i,j,k) &= -\frac{2\Delta t}{2\varepsilon_y(i,j,k) + \Delta t\sigma_y^e(i,j,k)}.
\end{aligned}
\tag{1.28}
$$

$$
\begin{aligned}
E_z^{n+1}(i,j,k) = {} & C_{eze}(i,j,k) \times E_z^n(i,j,k)\\
& + C_{ezhy}(i,j,k) \times \Big(H_y^{n+\frac{1}{2}}(i,j,k) - H_y^{n+\frac{1}{2}}(i-1,j,k)\Big)\\
& + C_{ezhx}(i,j,k) \times \Big(H_x^{n+\frac{1}{2}}(i,j,k) - H_x^{n+\frac{1}{2}}(i,j-1,k)\Big)\\
& + C_{ezj}(i,j,k) \times J_{iz}^{n+\frac{1}{2}}(i,j,k),
\end{aligned}
$$

where

$$
\begin{aligned}
C_{eze}(i,j,k) &= \frac{2\varepsilon_z(i,j,k) - \Delta t\sigma_z^e(i,j,k)}{2\varepsilon_z(i,j,k) + \Delta t\sigma_z^e(i,j,k)},\\
C_{ezhy}(i,j,k) &= \frac{2\Delta t}{\big(2\varepsilon_z(i,j,k) + \Delta t\sigma_z^e(i,j,k)\big)\Delta x},\\
C_{ezhx}(i,j,k) &= -\frac{2\Delta t}{\big(2\varepsilon_z(i,j,k) + \Delta t\sigma_z^e(i,j,k)\big)\Delta y},\\
C_{ezj}(i,j,k) &= -\frac{2\Delta t}{2\varepsilon_z(i,j,k) + \Delta t\sigma_z^e(i,j,k)}.
\end{aligned}
\tag{1.29}
$$

$$
\begin{aligned}
H_x^{n+\frac{1}{2}}(i,j,k) = {} & C_{hxh}(i,j,k) \times H_x^{n-\frac{1}{2}}(i,j,k)\\
& + C_{hxey}(i,j,k) \times \Big(E_y^n(i,j,k+1) - E_y^n(i,j,k)\Big)\\
& + C_{hxez}(i,j,k) \times \big(E_z^n(i,j+1,k) - E_z^n(i,j,k)\big)\\
& + C_{hxm}(i,j,k) \times M_{ix}^n(i,j,k),
\end{aligned}
$$

where

$$
\begin{aligned}
C_{hxh}(i,j,k) &= \frac{2\mu_x(i,j,k) - \Delta t\sigma_x^m(i,j,k)}{2\mu_x(i,j,k) + \Delta t\sigma_x^m(i,j,k)},\\
C_{hxey}(i,j,k) &= \frac{2\Delta t}{\big(2\mu_x(i,j,k) + \Delta t\sigma_x^m(i,j,k)\big)\Delta z},\\
C_{hxez}(i,j,k) &= -\frac{2\Delta t}{\big(2\mu_x(i,j,k) + \Delta t\sigma_x^m(i,j,k)\big)\Delta y},\\
C_{hxm}(i,j,k) &= -\frac{2\Delta t}{2\mu_x(i,j,k) + \Delta t\sigma_x^m(i,j,k)}.\\
H_y^{n+\frac{1}{2}}(i,j,k) &= C_{hyh}(i,j,k) \times H_y^{n-\frac{1}{2}}(i,j,k) + C_{hyez}(i,j,k)\\
&\quad \times \big(E_z^n(i+1,j,k) - E_z^n(i,j,k)\big) + C_{hyex}(i,j,k)\\
&\quad \times \big(E_x^n(i,j,k+1) - E_x^n(i,j,k)\big) + C_{hym}(i,j,k) \times M_{iy}^n(i,j,k)
\end{aligned}
\tag{1.30}
$$

where

$$
\begin{aligned}
C_{hyh}(i,j,k) &= \frac{2\mu_y(i,j,k) - \Delta t\sigma_y^m(i,j,k)}{2\mu_y(i,j,k) + \Delta t\sigma_y^m(i,j,k)},\\
C_{hyez}(i,j,k) &= \frac{2\Delta t}{\Big(2\mu_y(i,j,k) + \Delta t\sigma_y^m(i,j,k)\Big)\Delta x},\\
C_{byex}(i,j,k) &= -\frac{2\Delta t}{\Big(2\mu_y(i,j,k) + \Delta t\sigma_y^m(i,j,k)\Big)\Delta z},\\
C_{hym}(i,j,k) &= -\frac{2\Delta t}{2\mu_y(i,j,k) + \Delta t\sigma_y^m(i,j,k)}.\\
H_z^{n+\frac{1}{2}}(i,j,k) &= C_{hzh}(i,j,k) \times H_z^{n-\frac{1}{2}}(i,j,k)\\
&\quad + C_{hzex}(i,j,k) \times \big(E_x^n(i,j+1,k) - E_x^n(i,j,k)\big)\\
&\quad + C_{hzey}(i,j,k) \times \Big(E_y^n(i+1,j,k) - E_y^n(i,j,k)\Big)\\
&\quad + C_{hzm}(i,j,k) \times M_{iz}^n(i,j,k),
\end{aligned}
\tag{1.31}
$$

where

$$
\begin{aligned}
C_{hzh}(i,j,k) &= \frac{2\mu_y(i,j,k) - \Delta t\sigma_z^m(i,j,k)}{2\mu_z(i,j,k) + \Delta t\sigma_z^m(i,j,k)},\\
C_{hzex}(i,j,k) &= \frac{2\Delta t}{\big(2\mu_z(i,j,k) + \Delta t\sigma_z^m(i,j,k)\big)\Delta y},\\
C_{hzey}(i,j,k) &= -\frac{2\Delta t}{\big(2\mu_z(i,j,k) + \Delta t\sigma_z^m(i,j,k)\big)\Delta x},\\
C_{hzm}(i,j,k) &= -\frac{2\Delta t}{2\mu_z(i,j,k) + \Delta t\sigma_z^m(i,j,k)}.
\end{aligned}
$$

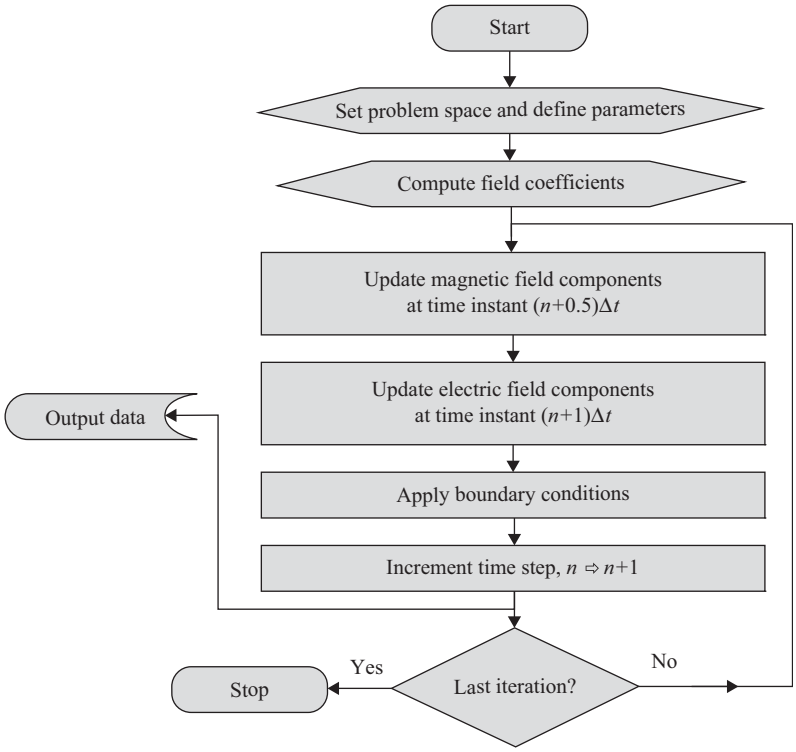

Figure 1.9 Explicit FDTD procedure.

It should be noted that the first two subscripts in each coefficient refer to the corresponding field component being updated. For three subscripts coefficients, the third subscript refers to the type of the field or source (electric or magnetic) that this coefficient is multiplied by. For four subscripts coefficients, the third and fourth subscripts refer to the type of the field that this coefficient is multiplied by.

Having derived the FDTD updating equations, a time-marching algorithm can be constructed as illustrated in Figure 1.9. The first step in this algorithm is setting up the problem space – including the objects, material types, and sources – and defining any other parameters that will be used during the FDTD computation. Then the coefficient terms appearing in (1.26)–(1.31) can be calculated and stored as arrays before the iteration is started. The field components need to be defined as arrays as well and shall be initialized with zeros since the initial values of the fields in the problem space in most cases are zeros, and fields will be induced in the problem space due to sources as the iteration proceeds. At every step of the time-marching iteration the magnetic field components are updated for time instant $(n + 0.5)\Delta t$ using (1.29)–(1.31); then the electric field components are updated for time instant $(n + 1)\Delta t$ using (1.26)–(1.28). The problem space has a finite size, and specific boundary conditions can be enforced on the boundaries of the problem space. Therefore, the field components on the boundaries of the problem space are treated according to the type of boundary conditions during the iteration. The types of boundary conditions and the

techniques used to integrate them into the FDTD algorithm are discussed in detail in Chapters 7 and 8. After the fields are updated and boundary conditions are enforced, the current values of any desired field components can be captured and stored as output data, and these data can be used for real-time processing or postprocessing to calculate some other desired parameters. The FDTD iterations can be continued until some stopping criteria are achieved.

1.4 FDTD updating equations for two-dimensional problems

The FDTD updating equations given in (1.26)–(1.31) can be used to solve three-dimensional problems. In the two-dimensional case where there is no variation in the problem geometry and field distributions in one of the dimensions, a simplified set of updating equations can be obtained starting from the Maxwell's curl equations system (1.4). Since there is no variation in one of the dimensions, the derivative terms with respect to that dimension vanish. For instance, if the problem is z dimension independent, equations (1.4) reduce to

$$\frac{\partial E_x}{\partial t} = \frac{1}{\varepsilon_x}\left(\frac{\partial H_z}{\partial y} - \sigma_x^e E_x - J_{ix}\right), \tag{1.32a}$$

$$\frac{\partial E_y}{\partial t} = \frac{1}{\varepsilon_y}\left(-\frac{\partial H_z}{\partial x} - \sigma_y^e E_y - J_{iy}\right), \tag{1.32b}$$

$$\frac{\partial E_z}{\partial t} = \frac{1}{\varepsilon_z}\left(\frac{\partial H_y}{\partial x} - \frac{\partial H_x}{\partial y} - \sigma_z^e E_z - J_{iz}\right), \tag{1.32c}$$

$$\frac{\partial H_x}{\partial t} = \frac{1}{\mu_x}\left(-\frac{\partial E_z}{\partial y} - \sigma_x^m H_x - M_{ix}\right), \tag{1.32d}$$

$$\frac{\partial H_y}{\partial t} = \frac{1}{\mu_y}\left(\frac{\partial E_z}{\partial x} - \sigma_y^m H_y - M_{iy}\right), \tag{1.32e}$$

$$\frac{\partial H_z}{\partial t} = \frac{1}{\mu_z}\left(\frac{\partial E_x}{\partial y} - \frac{\partial E_y}{\partial x} - \sigma_z^m H_z - M_{iz}\right). \tag{1.32f}$$

One should notice that equations (1.32a), (1.32b), and (1.32f) are dependent only on the terms E_x, E_y, and H_z, whereas equations (1.32c), (1.32d), and (1.32e) are dependent only on the terms E_z, H_x, and H_y. Therefore, the six equations (1.32) can be treated as two separate sets of equations. In the first set (1.32a), (1.32b), and (1.32f) – all the electric field components are transverse to the reference dimension z; therefore, this set of equations constitutes the transverse electric to z case – TE_z. In the second set – (1.32c), (1.32d), and (1.32e) – all the magnetic field components are transverse to the reference dimension z; therefore, this set of equations constitutes the transverse magnetic to z case – TM_z. Most two-dimensional problems can be decomposed into two separate problems, each including separate field components that are TE_z and TM_z for the case under consideration. These two problems can be solved separately, and the solution for the main problem can be achieved as the sum of the two solutions.

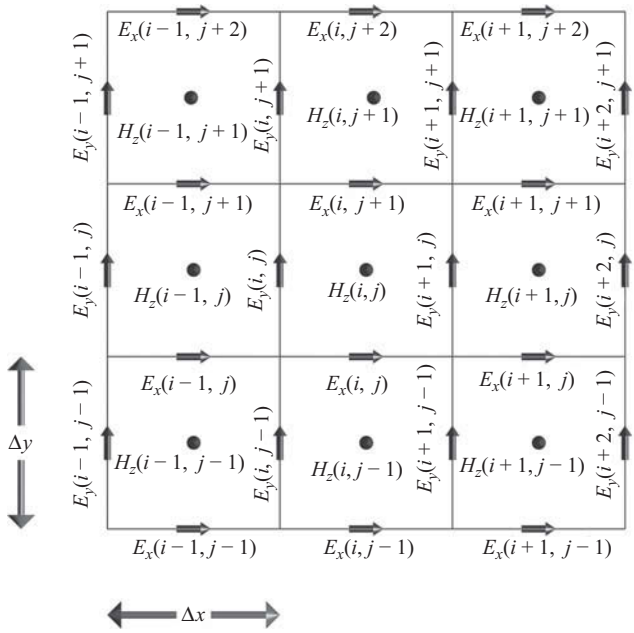

Figure 1.10 Two-dimensional TE_z FDTD field components.

The FDTD updating equations for the TE_z case can be obtained by applying the central difference formula to the equations constituting the TE_z case based on the field positions shown in Figure 1.10, which is obtained by projection of the Yee cells in Figure 1.5 on the xy plane in the z direction. The FDTD updating equations for the TE_z case are therefore obtained as

$$E_x^{n+1}(i,j) = C_{exe}(i,j) \times E_x^n(i,j) + C_{exhz}(i,j) \times \left(H_z^{n+\frac{1}{2}}(i,j) - H_z^{n+\frac{1}{2}}(i,j-1)\right) + C_{exj}(i,j) \times J_{ix}^{n+\frac{1}{2}}(i,j), \tag{1.33}$$

where

$$C_{exe}(i,j) = \frac{2\varepsilon_x(i,j) - \Delta t\sigma_x^e(i,j)}{2\varepsilon_x(i,j) + \Delta t\sigma_x^e(i,j)},$$

$$C_{exhz}(i,j) = \frac{2\Delta t}{\left(2\varepsilon_x(i,j) + \Delta t\sigma_x^e(i,j)\right)\Delta y},$$

$$C_{exj}(i,j) = -\frac{2\Delta t}{2\varepsilon_x(i,j) + \Delta t\sigma_x^e(i,j)}.$$

$$E_y^{n+1}(i,j) = C_{eye}(i,j) \times E_y^n(i,j) + C_{eyhz}(i,j) \times \left(H_z^{n+\frac{1}{2}}(i,j) - H_z^{n+\frac{1}{2}}(i-1,j)\right) + C_{eyj}(i,j) \times J_{iy}^{n+\frac{1}{2}}(i,j), \tag{1.34}$$

where

$$
\begin{aligned}
C_{eye}(i,j) &= \frac{2\varepsilon_y(i,j) - \Delta t\sigma_y^e(i,j)}{2\varepsilon_y(i,j) + \Delta t\sigma_y^e(i,j)},\\
C_{eyhz}(i,j) &= -\frac{2\Delta t}{\left(2\varepsilon_y(i,j) + \Delta t\sigma_y^e(i,j)\right)\Delta x},\\
C_{eyj}(i,j) &= -\frac{2\Delta t}{2\varepsilon_y(i,j) + \Delta t\sigma_y^e(i,j)}.\\
H_z^{n+\frac{1}{2}}(i,j) &= C_{hzh}(i,j) \times H_z^{n-\frac{1}{2}}(i,j) + C_{bzex}(i,j) \times \left(E_x^n(i,j+1) - E_x^n(i,j)\right)\\
&\quad + C_{hzey}(i,j) \times \left(E_y^n(i+1,\, j) - E_y^n(i,j)\right) + C_{hzm}(i,j) \times M_{iz}^m(i,j),
\end{aligned}
\tag{1.35}
$$

where

$$
\begin{aligned}
C_{hzh}(i,j) &= \frac{2\mu_z(i,\, j) - \Delta t\sigma_z^m(i,\, j)}{2\mu_z(i,\, j) + \Delta t\sigma_z^m(i,\, j)},\\
C_{hzex}(i,j) &= \frac{2\Delta t}{\left(2\mu_z(i,\, j) + \Delta t\sigma_z^m(i,\, j)\right)\Delta y},\\
C_{hzey}(i,j) &= -\frac{2\Delta t}{\left(2\mu_z(i,j) + \Delta t\sigma_z^m(i,j)\right)\Delta x},\\
C_{hzm}(i,j) &= -\frac{2\Delta t}{2\mu_z(i,j) + \Delta t\sigma_z^m(i,j)}.
\end{aligned}
$$

Since the FDTD updating equations for the three-dimensional case are readily available, they can be used to derive (1.33), (1.34), and (1.35) by simply setting the coefficients including $1/\Delta z$ to zero. Hence, the FDTD updating equations for the TM_z case can be obtained by eliminating the term $C_{hxey}(i, j, k)$ in (1.29) and eliminating the term $C_{hyex}(i, j, k)$ in (1.30) based on the field positions shown in Figure 1.11, such that

$$
\begin{aligned}
E_z^{n+1}(i,j) &= C_{eze}(i,j) \times E_z^n(i,j) + C_{ezhy}(i,j) \times \left(H_y^{n+\frac{1}{2}}(i,j) - H_y^{n+\frac{1}{2}}(i-1,j)\right)\\
&\quad + C_{ezhx}(i,j) \times \left(H_x^{n+\frac{1}{2}}(i,j) - H_x^{n+\frac{1}{2}}(i,j-1)\right) + C_{ezj}(i,j) \times J_{iz}^{n+\frac{1}{2}}(i,j),
\end{aligned}
\tag{1.36}
$$

where

$$
\begin{aligned}
C_{eze}(i,j) &= \frac{2\varepsilon_z(i,j) - \Delta t\sigma_z^e(i,j)}{2\varepsilon_z(i,j) + \Delta t\sigma_z^e(i,j)},\\
C_{ezhy}(i,j) &= \frac{2\Delta t}{\left(2\varepsilon_z(i,j) + \Delta t\sigma_z^e(i,j)\right)\Delta x},\\
C_{ezhx}(i,j) &= -\frac{2\Delta t}{\left(2\varepsilon_z(i,j) + \Delta t\sigma_z^e(i,j)\right)\Delta y},\\
C_{ezj}(i,j) &= -\frac{2\Delta t}{2\varepsilon_z(i,j) + \Delta t\sigma_z^e(i,j)}.\\
H_x^{n+\frac{1}{2}}(i,j) &= C_{hxh}(i,j) \times H_x^{n-\frac{1}{2}}(i,j) + C_{hxez}(i,j) \times \left(E_z^n(i,j+1) - E_z^n(i,j)\right)\\
&\quad + C_{hxm}(i,j) \times M_{ix}^n(i,j),
\end{aligned}
\tag{1.37}
$$

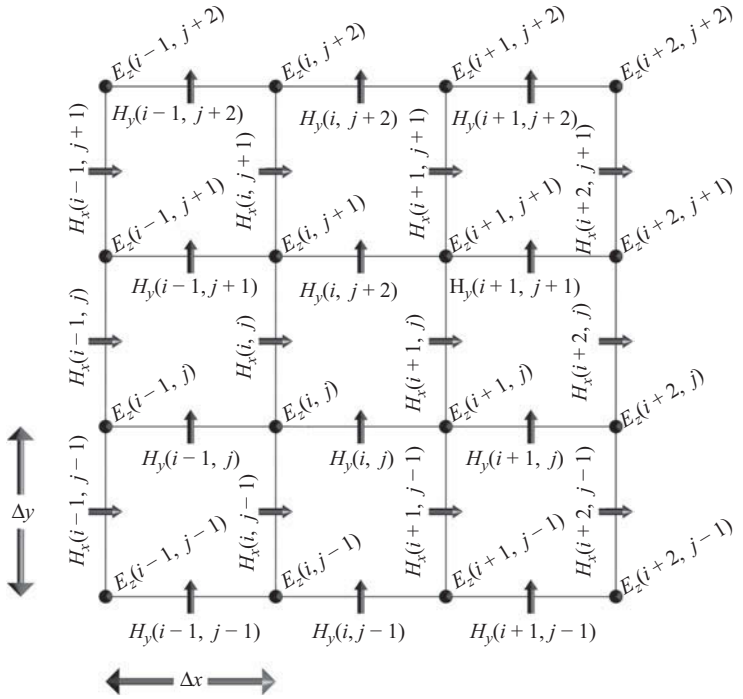

Figure 1.11 Two-dimensional TM_z FDTD field components.

where

$$
\begin{aligned}
C_{hxh}(i,j) &= \frac{2\mu_x(i,j) - \Delta t\sigma_x^m(i,j)}{2\mu_x(i,j) + \Delta t\sigma_x^m(i,j)},\\
C_{hxez}(i,j) &= -\frac{2\Delta t}{\big(2\mu_x(i,j) + \Delta t\sigma_x^m(i,j)\big)\Delta y},\\
C_{hxm}(i,j) &= -\frac{2\Delta t}{2\mu_x(i,j) + \Delta t\sigma_x^m(i,j)}.\\
H_y^{n+\frac{1}{2}}(i,j) &= C_{hyh}(i,j) \times H_y^{n-\frac{1}{2}}(i,j) + C_{hyez}(i,j) \times \big(E_z^n(i+1,j) - E_z^n(i,j)\big)\\
&\quad + C_{hym}(i,j) \times M_{iy}^m(i,j),
\end{aligned}
\tag{1.38}
$$

where

$$
\begin{aligned}
C_{hyh}(i,j) &= \frac{2\mu_y(i,j) - \Delta t\sigma_y^m(i,j)}{2\mu_y(i,j) + \Delta t\sigma_y^m(i,j)},\\
C_{hyez}(i,j) &= \frac{2\Delta t}{\Big(2\mu_y(i,j) + \Delta t\sigma_y^m(i,j)\Big)\Delta x},\\
C_{hym}(i,j) &= -\frac{2\Delta t}{2\mu_y(i,j) + \Delta t\sigma_y^m(i,j)}.
\end{aligned}
$$

1.5 FDTD updating equations for one-dimensional problems

In the one-dimensional case, there is no variation in the problem geometry and field distributions in two of the dimensions. For instance, if the y and z dimensions have no variation, the derivative with respect to the y and z dimensions vanish in Maxwell's curl equations. Therefore, the two-dimensional curl equations (1.32a)–(1.32f) reduce to

$$\frac{\partial E_x}{\partial t} = \frac{1}{\varepsilon_x}\left(-\sigma_x^e E_x - J_{ix}\right), \tag{1.39a}$$

$$\frac{\partial E_y}{\partial t} = \frac{1}{\varepsilon_y}\left(-\frac{\partial H_z}{\partial x} - \sigma_y^e E_y - J_{iy}\right), \tag{1.39b}$$

$$\frac{\partial E_z}{\partial t} = \frac{1}{\varepsilon_z}\left(\frac{\partial H_y}{\partial x} - \sigma_z^e E_z - J_{iz}\right), \tag{1.39c}$$

$$\frac{\partial H_x}{\partial t} = \frac{1}{\mu_x}\left(-\sigma_x^m H_x - M_{ix}\right), \tag{1.39d}$$

$$\frac{\partial H_y}{\partial t} = \frac{1}{\mu_y}\left(\frac{\partial E_z}{\partial x} - \sigma_y^m H_y - M_{iy}\right), \tag{1.39e}$$

$$\frac{\partial H_z}{\partial t} = \frac{1}{\mu_z}\left(-\frac{\partial E_y}{\partial x} - \sigma_z^m H_z - M_{iz}\right). \tag{1.39f}$$

It should be noted that (1.39a) and (1.39d) include time derivatives but not space derivatives. Therefore, these equations do not represent propagating fields, hence the field components E_x and H_x, which only exist in these two equations, do not propagate. The other four equations represent propagating fields, and both the electric and magnetic field components existing in these equations are transverse to the x dimension. Therefore, transverse electric and magnetic to x (TEM_x) fields exist and propagate as plane waves in the one-dimensional case under consideration.

Similar to the two-dimensional case, the one-dimensional case as well can be decomposed into two separate cases, since (1.39b) and (1.39f), which include only the terms E_y and H_z, are decoupled from (1.39c) and (1.39e), which include only the terms E_z and H_y. FDTD updating equations can be obtained for (1.39b) and (1.39f) using the central difference formula based on the field positioning in one-dimensional space as illustrated in Figure 1.12, such that

$$E_y^{n+1}(i) = C_{eye}(i) \times E_y^n(i) + C_{eyhz}(i) \times \left(H_z^{n+\frac{1}{2}}(i) - H_z^{n+\frac{1}{2}}(i-1)\right) + C_{eyj}(i) \times J_{iy}^{n+\frac{1}{2}}(i), \tag{1.40}$$

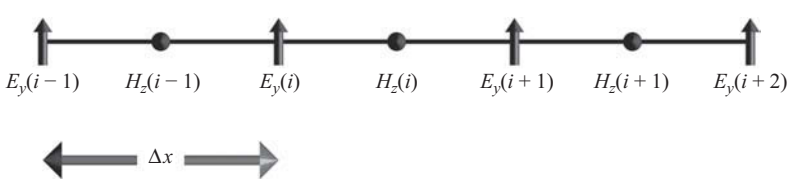

Figure 1.12 One-dimensional FDTD – positions of field components E_y and H_z.

where

$$C_{eye}(i) = \frac{2\varepsilon_y(i) - \Delta t\sigma_y^e(i)}{2\varepsilon_y(i) + \Delta t\sigma_y^e(i)},$$
$$C_{eyhz}(i) = -\frac{2\Delta t}{\left(2\varepsilon_y(i) + \Delta t\sigma_y^e(i)\right)\Delta x},$$
$$C_{eyj}(i) = -\frac{2\Delta t}{2\varepsilon_y(i) + \Delta t\sigma_y^e(i)},$$

and

$$H_z^{n+\frac{1}{2}}(i) = C_{hzh}(i) \times H_z^{n-\frac{1}{2}}(i) + C_{hzey}(i) \times \left(E_y^n(i+1) - E_y^n(i)\right) + C_{hzm}(i) \times M_{iz}^n(i), \quad (1.41)$$

where

$$C_{hzh}(i) = \frac{2\mu_z(i) - \Delta t\sigma_z^m(i)}{2\mu_z(i) + \Delta t\sigma_z^m(i)},$$
$$C_{hzey}(i) = -\frac{2\Delta t}{\left(2\mu_z(i) + \Delta t\sigma_z^m(i)\right)\Delta x},$$
$$C_{hzm}(i) = -\frac{2\Delta t}{2\mu_z(i) + \Delta t\sigma_z^m(i)}.$$

Similarly, FDTD updating equations can be obtained for (1.39c) and (1.39e) using the central difference formula based on the field positioning in one-dimensional space as illustrated in Figure 1.13, such that

$$E_z^{n+1}(i) = C_{eze}(i) \times E_z^n(i) + C_{ezhy}(i) \times \left(H_y^{n+\frac{1}{2}}(i) - H_y^{n+\frac{1}{2}}(i-1)\right) + C_{ezj}(i) \times J_{iz}^{n+\frac{1}{2}}(i), \quad (1.42)$$

where

$$C_{eze}(i) = \frac{2\varepsilon_z(i) - \Delta t\sigma_z^e(i)}{2\varepsilon_z(i) + \Delta t\sigma_z^e(i)},$$
$$C_{ezhy}(i) = \frac{2\Delta t}{\left(2\varepsilon_z(i) + \Delta t\sigma_z^e(i)\right)\Delta x},$$
$$C_{ezj}(i) = -\frac{2\Delta t}{2\varepsilon_z(i) + \Delta t\sigma_z^e(i)},$$

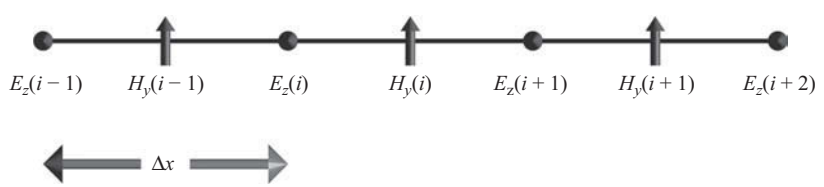

Figure 1.13 One-dimensional FDTD – positions of field components E_z and H_y.

and

$$H_y^{n+\frac{1}{2}}(i) = C_{hyh}(i) \times H_y^{n-\frac{1}{2}}(i) + C_{hyez}(i) \times \left(E_z^n(i+1) - E_z^n(i)\right) + C_{hym}(i) \times M_{iy}^n(i), \quad (1.43)$$

where

$$C_{hyh}(i) = \frac{2\mu_y(i) - \Delta t \sigma_y^m(i)}{2\mu_y(i) + \Delta t \sigma_y^m(i)},$$

$$C_{hyez}(i) = \frac{2\Delta t}{\left(2\mu_y(i) + \Delta t \sigma_y^m(i)\right)\Delta x},$$

$$C_{hym}(i) = -\frac{2\Delta t}{2\mu_y(i) + \Delta t \sigma_y^m(i)}.$$

A MATLAB code is given in Appendix A for a one-dimensional FDTD implementation based on the updating equations (1.42) and (1.43). The code calculates electric and magnetic field components generated by a z-directed current sheet, J_z, placed at the center of a problem space filled with air between two parallel, perfect electric conductor (PEC) plates extending to infinity in the y and z dimensions. Figure 1.14 shows snapshots of E_z and H_y within the FDTD computational domain demonstrating the propagation of the fields and their reflection from the PEC plates at the left and right boundaries.

In the demonstrated problem, the parallel plates are 1 m apart. The one-dimensional problem space is represented by cells having width $\Delta x = 1$ mm. The current sheet at the center excites a current with 1 A/m^2 density and Gaussian waveform

$$J_z(t) = e^{-\left(\frac{t-2\times10^{-10}}{5\times10^{-11}}\right)^2}.$$

The current sheet is excited over a one-cell cross-section (i.e., 1 mm wide), which translates J_z into a surface current density K_z of magnitude 1×10^{-3} A/m. The surface current density causes a discontinuity in magnetic field and generates H_y, which satisfies the boundary condition $\vec{K} = \hat{n} \times \vec{H}$. Therefore, two waves of H_y are generated on both sides of the current sheet, each of which has magnitude 5×10^{-4} A/m. Since the fields are propagating in free space, the magnitude of the generated electric field is $\eta_0 \times 5 \times 10^{-4} \approx 0.1885$ V/m, where η_0 is the intrinsic impedance of free space ($\eta_0 \approx 377$).

Examining the listing of the one-dimensional FDTD code in Appendix A, one immediately notices that the sizes of the arrays associated with E_z and H_y are not the same. The one-dimensional problem space is divided into nx intervals; therefore, there are $nx + 1$ *nodes* in the problem space including the left and right boundary nodes. This code is based on the field positioning scheme given in Figure 1.13, where the E_z components are defined at node positions and the H_y components are defined at the center positions of the intervals. Therefore, arrays associated with E_z have the size $nx + 1$, whereas those associated with H_y have the size nx.

Another point that deserves consideration is the application of the boundary conditions. In this problem the boundaries are PEC; thus, the tangential electric field component (E_z in this case) vanishes on the PEC surface. Therefore, this condition can be enforced on the electric field component on the boundaries, $E_z(1)$ and $E_z(nx + 1)$, as can be seen in the

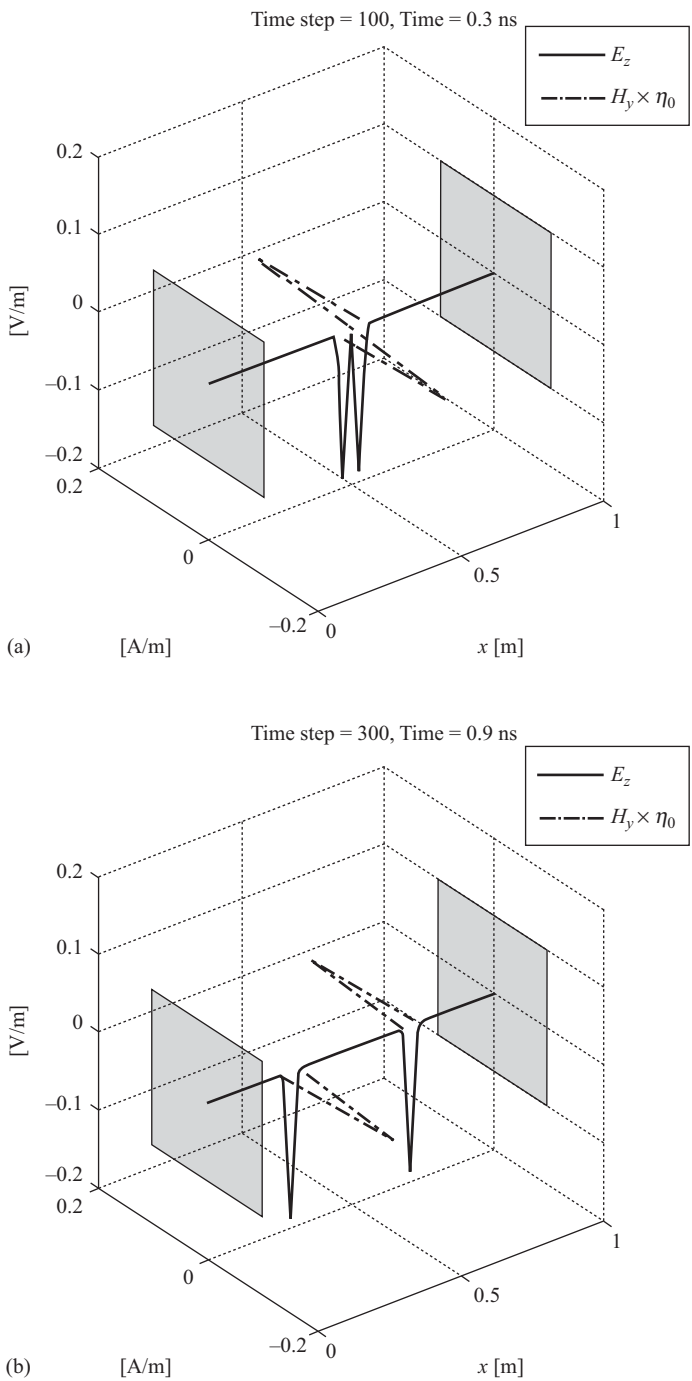

Figure 1.14 Snapshots of a one-dimensional FDTD simulation: (a) fields observed after 100 time steps; (b) fields observed after 300 time steps; (c) fields observed after 615 time steps; and (d) fields observed after 700 time steps.

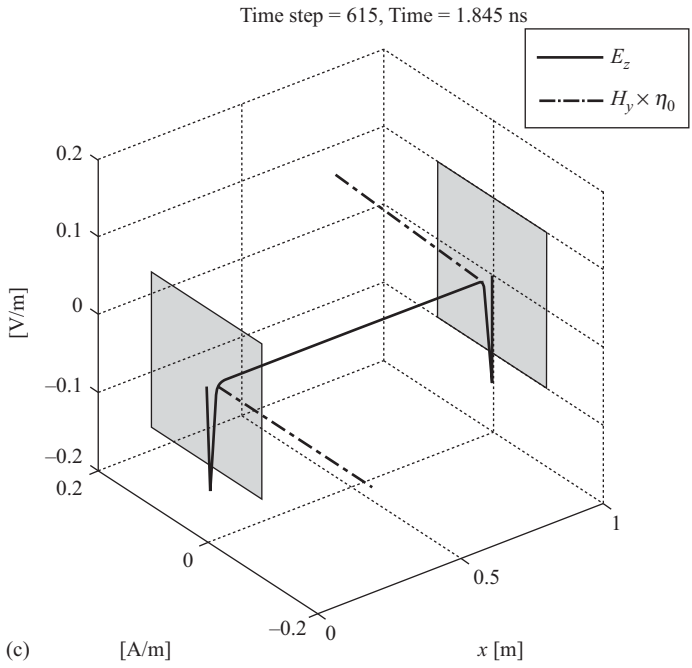

(c)

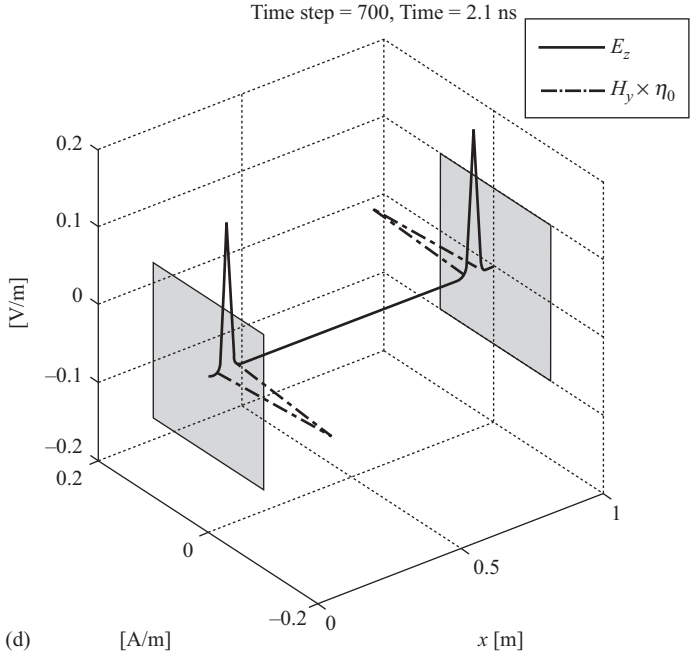

(d)

Figure 1.14 (*Continued*)

code listing. Observing the changes in the fields from time step 650 to 700 in Figure 1.14 reveals the correct behavior of the incident and reflected waves for a PEC plate. This is evident by the reversal of the direction of the peak value of E_z after reflection from the PEC boundaries, which represents a reflection coefficient equal to -1 while the behavior of the reflected H_y component represents the reflection coefficient that is equal to $+1$ as expected.

1.6 Exercises

1.1 Follow the steps presented in Section 1.2 to develop the appropriate approximations for the first derivative of a function with second-order accuracy using the forward and backward difference procedure and fourth-order accuracy using the central difference procedure. Compare your derived expressions with those listed in Table 1.1.

1.2 Update the MATLAB program in Listing 1.1 to regenerate Figure 1.2 using the second-order accurate forward and backward differences and the fourth-order accurate central difference approximations for the same function.

1.3 Update the MATLAB program in Listing 1.1 to generate the corresponding figures to Figure 1.2, but for the second derivatives of the function. Use the approximate expressions in the right column of Table 1.1 while updating the program.

1.4 The steps of the development of the updating equation for the x component of the electric field are demonstrated in Section 1.3. Follow the same procedure to show the steps required to develop the updating equations for the y and z components for the electric field. Pay sufficient attention to the selection of the indices of each individual field component in your expressions. The Yee cell presented in Figure 1.5 should help you in understanding the proper use of these indices.

1.5 Repeat Exercise 1.4, but this time for developing the updating equations for the magnetic field components.